Fractionation of 226Ra and Ba in the Upper North Pacific Ocean

Pieter van Beek, Roger François, Makio Honda, Matthew A Charette, Jean-Louis Reyss, Raja Ganeshram, Christophe Monnin, Susumu Honjo

frontiers | Frontiers in Marine Science

ORIGINAL RESEARCH
published: 15 July 2022
doi: 10.3389/fmars.2022.859117

Fractionation of ^{226}Ra and Ba in the Upper North Pacific Ocean

Pieter van Beek[1], Roger François[2], Makio Honda[3], Matthew A. Charette[4], Jean-Louis Reyss[5], Raja Ganeshram[6], Christophe Monnin[7] and Susumu Honjo[4†]*

[1] Laboratoire d'Etudes en Géophysique et Océanographie Spatiales (LEGOS), Université de Toulouse, CNES/CNRS/IRD/ Université Toulouse III Paul Sabatier, Toulouse, France, [2] Department of Earth, Ocean, and Atmospheric Sciences, University of British Columbia, Vancouver, BC, Canada, [3] Department of Environmental Geochemical Cycle Research (DEGCR), Japan Agency for Marine-Earth Science and Technology (JAMSTEC), Yokosuka, Japan, [4] Department of Marine Chemistry and Geochemistry, Woods Hole Oceanographic Institution, WoodsHole, MA, United States, [5] Laboratoire des Sciences du Climat et de l'Environnement, Gif-sur-Yvette, France, [6] School of Geosciences, Grant Institute, University of Edinburgh, Edinburgh, United Kingdom, [7] Géosciences Environnement Toulouse (CNRS/UPS/IRD/CNES), Observatoire Midi Pyrénées, Toulouse, France

OPEN ACCESS

Edited by:
Paul Mcginnity, IAEA International Atomic Energy Agency, Monaco

Reviewed by:
Zvi Steiner, Helmholtz Association of German Research Centres (HZ), Germany
Frank Dehairs, Vrije University Brussel, Belgium

***Correspondence:**
Pieter van Beek
vanbeek@legos.obs-mip.fr

[†]Deceased

Specialty section:
This article was submitted to Ocean Observation, a section of the journal Frontiers in Marine Science

Received: *20 January 2022*
Accepted: *25 May 2022*
Published: *15 July 2022*

Citation:
van Beek P, François R, Honda M, Charette MA, Reyss J-L, Ganeshram R, Monnin C and Honjo S (2022) Fractionation of ^{226}Ra and Ba in the Upper North Pacific Ocean. Front. Mar. Sci. 9:859117. doi: 10.3389/fmars.2022.859117

Investigations conducted during the GEOSECS program concluded that radium-226 ($T_{1/2}$ = 1602 y) and barium are tightly correlated in waters above 2500 m in the Atlantic, Pacific and Antarctic Oceans, with a fairly uniform ^{226}Ra/Ba ratio of 2.3 ± 0.2 dpm µmol^{-1} (4.6 nmol ^{226}Ra/mol Ba). Here, we report new ^{226}Ra and Ba data obtained at three different stations in the Pacific Ocean: stations K1 and K3 in the North-West Pacific and station old Hale Aloha, off Hawaii Island. The relationship between ^{226}Ra and Ba found at these stations is broadly consistent with that reported during the GEOSECS program. At the three investigated stations, however, we find that the ^{226}Ra/Ba ratios are significantly lower in the upper 500 m of the water column than at greater depths, a pattern that was overlooked during the GEOSECS program, either because of the precision of the measurements or because of the relatively low sampling resolution in the upper 500 m. Although not always apparent in individual GEOSECS profiles, this trend was noted before from the non-zero intercept of the linear regression when plotting the global data set of Ba versus ^{226}Ra seawater concentration and was attributed, at least in part, to the predominance of surface input from rivers for Ba versus bottom input from sediments for ^{226}Ra. Similarly, low ^{226}Ra/Ba ratios in the upper 500 m have been reported in other oceanic basins (e.g. Atlantic Ocean). Parallel to the low ^{226}Ra/Ba ratios in seawater, higher ^{226}Ra/Ba ratios were found in suspended particles collected in the upper 500 m. This suggests that fractionation between the two elements may contribute to the lower ^{226}Ra/Ba ratios found in the upper 500 m, with ^{226}Ra being preferentially removed from surface water, possibly as a result of mass fractionation during celestite formation by acantharians and/or barite precipitation, since both chemical elements have similar ionic radius and the same configuration of valence electrons. This finding has implications for dating of marine carbonates by ^{226}Ra, which requires a constant initial ^{226}Ra/Ba ratio incorporated in the shells and for using ^{226}Ra as an abyssal circulation and mixing tracer.

Keywords: radium, barium, seawater, ratio, fractionation, dating, ocean circulation, suspended particles

INTRODUCTION

Seawater radium (Ra) and barium (Ba) distributions were measured extensively in all major ocean basins during the GEOSECS program (Broecker et al., 1967; Wolgemuth and Broecker, 1970; Bacon and Edmond, 1972; Broecker et al., 1976; Chan et al., 1976; Ku and Lin, 1976; Chung and Craig, 1980; Ku et al., 1980) and more recently during the GEOTRACES program (see e.g. Le Roy et al., 2018). Because of their similar chemical properties, it was argued that Ba and ^{226}Ra would not be biologically fractionated and that ^{226}Ra/Ba ratios would only be affected by the decay of ^{226}Ra, providing an independent clock that would complement the information obtained from ^{14}C/^{12}C ratios to yield important constraints on the circulation and mixing of abyssal waters (e.g. Ku and Luo, 1994). The GEOSECS data showed that ^{226}Ra and Ba are linearly correlated over much of the water column in the Atlantic, Pacific and Indian Oceans (**Figure 1 of the Supplementary Material**), resulting in a fairly constant ^{226}Ra/Ba ratio of 2.3 ± 0.2 dpm μmol^{-1} or 4.6 nmol mol^{-1} (Li et al., 1973; Chan et al., 1976; Ku et al., 1980; Foster et al., 2004). Several factors, however, have complicated the use of ^{226}Ra/Ba as a large scale abyssal circulation and mixing tracer. The source of Ba, which is added mainly to the upper ocean by rivers and submarine groundwater discharge, is different from the source of ^{226}Ra, which has a significant oceanic source through diffusion from deep-sea sediments. As a result, the linear correlation between Ba and ^{226}Ra breaks down in near-bottom waters, where ^{226}Ra activities are significantly higher than predicted from the radium-barium relationship (Chung, 1974; Chan et al., 1976; Chung and Craig, 1980; Ku et al., 1980; Rhein and Schlitzer, 1988). Furthermore, the rate of ^{226}Ra diffusion from the bottom is variable and depends on particle settling flux and mineral dissolution on the seafloor, which dictate the ^{230}Th concentration of the sediment that generates ^{226}Ra by decay (Chan et al., 1976; Chung, 1976). Likewise, an inherent assumption when using ^{226}Ra/Ba as a circulation/mixing tracer is that biological recycling does not fractionate Ba and Ra, i.e. they are taken up and released in the same ratio at which they are found in seawater. This assumption, however, has never been rigorously verified (Ku and Luo, 1994).

The increasing concentration of ^{226}Ra and Ba from the surface to the deep ocean indicates that these elements are removed from surface seawater by sinking particles and released back to seawater at depth. Ku and Luo (1994) argue that most of the release happens on the seafloor rather than from sinking particles. Uptake of Ba and ^{226}Ra in the upper water column may occur through substitution for calcium in calcareous skeletons (Lea and Boyle, 1989; Lea and Boyle, 1990), adsorption onto diatom frustules or Fe hydroxides (Bishop, 1988; Ganeshram et al., 2003; Sternberg et al., 2005), substitution for Sr in celestite skeletons produced by acantharians (Bernstein et al., 1987; Bernstein et al., 1992; Jacquet et al., 2007) and barite ($BaSO_4$) precipitation (Chow and Goldberg, 1960; Dehairs et al., 1980; Bishop, 1988; Dehairs et al., 1990; Dehairs et al., 1991; Stroobants et al., 1991). Barite crystals are generally viewed as the most important Ba and Ra carriers in the water column (Dehairs et al., 1980; Dehairs et al., 1990; Moore and Dymond, 1991; Legeleux and Reyss, 1996). The observation of higher particulate Ba concentrations in the mesopelagic layer (ca. 200-600 m) thus led to conclude that barite predominantly forms in this depth interval (e.g. Dehairs et al., 1980), a pattern that was confirmed by the study of the ^{228}Ra/^{226}Ra signature of sinking particles (Legeleux and Reyss, 1996) and more recently by the analysis of barium stable isotopes (Horner et al., 2015; Hsieh and Hendersom, 2017).

Although the exact mechanism of barite formation in seawater is still not fully understood, it is generally accepted that barite precipitates in subsurface waters within supersaturated microenvironments that result from the decay of organic matter exported from the euphotic layer (Chow and Goldberg, 1960; Dehairs et al., 1980; Bishop, 1988; Stroobants et al., 1991; Legeleux and Reyss, 1996). Biogenic aggregates are thus considered as the necessary substrate for barite formation, a feature that was also confirmed by *in vitro* experiments (Ganeshram et al., 2003; Gonzales-Munoz et al., 2003; Sternberg et al., 2005). The observed relationship between particulate Ba (predominantly barite), oxygen and pCO_2 concentrations in the water column highlighted the potential role of bacteria in barite precipitation (Dehairs et al., 1990; Dehairs et al., 2008; Jacquet et al., 2011). More recently, it was shown that extracellular polymeric substances (EPS) - that are known to bind many chemical elements - could serve as nucleation sites that favor Ba accumulation, thus leading to the saturated microenvironment required for barite precipitation in undersaturated waters (Martinez-Ruiz et al., 2020). Alternatively, the high Ba concentrations found in celestite ($SrSO_4$) skeletons produced by acantharians led to the suggestion that the dissolution of these highly soluble skeletons could contribute to barite formation by releasing Ba and sulfate in the microenvironment of settling particles (Bernstein et al., 1987; Bernstein et al., 1992; Bernstein et al., 1998; Bernstein and Byrne, 2004).

Finally, in addition to being a useful tracer of ocean circulation and mixing, ^{226}Ra - with a half-life of 1602 y - has been used for dating marine samples within the Holocene epoch (eg., Schmidt and Cochran, 2010). In particular, the decay of ^{226}Ra incorporated in barite has been used to derive sedimentation rates in deep-sea sediments (Paytan et al., 1996; van Beek and Reyss, 2001; van Beek et al., 2002; van Beek et al., 2004) and to provide estimates of past sea-surface reservoir ages by comparing ages deduced from ^{226}Ra activities in barite and ^{14}C ages derived from planktic foraminifers (van Beek et al., 2002). Likewise, carbonate minerals can be dated by assuming that they acquire their initial ^{226}Ra/Ba ratio from ambient seawater (Berkman and Ku, 1998; Staubwasser et al., 2004). The accuracy of these dating methods, however, relies on knowing the initial ^{226}Ra activity (or initial ^{226}Ra/Ba ratio) incorporated in the samples and on their constancy over the dating period (i.e. the Holocene).

In this work, we report vertical profiles of ^{226}Ra, Ba and ^{226}Ra/Ba from three different locations in the Pacific Ocean (stations K1 and K3 in the North-West Pacific and old station Hale Aloha, off Hawaii) to better assess the variability of ^{226}Ra/Ba in seawater. We also document the underlying causes for the observed variations by i) conducting leaching experiments on the suspended particles that aim at characterizing the different Ba carriers in the

water column, ii) characterizing the saturation state of the water column with respect to barite and iii) studying the Ra isotopic signature (^{228}Ra/^{226}Ra) of the suspended particles to provide information on the depth of particulate Ba formation and transport in the water column.

MATERIAL AND METHODS

Study Sites

Samples were collected in the North-West Pacific in December 2002 on board RV Mirai, as part of the JPAC program (PIs: Makio Honda and Susumu Honjo) at station K1 (51°N-165°E; 5,130 m) in the Western Subarctic Gyre and at station K3 (39°N-160°E; 5,470 m) usually located north of the Kuroshio Front (**Figure 1**). We also report data on samples collected at old station Hale Aloha (22°28'N; 158°8' W) located north of Hawaii in June 2002 on board RV *Ka'imikai-o-Kanaloa* (*KoK)* and in August 2002 on board RV Wecoma (PI: Mike Bacon). This station is located south of station ALOHA that is the site of the Hawaii Ocean Time-series program (HOT, 22.75°N; 158.00°W). These sites off Hawaii are oligotrophic (low macronutrient and therefore low chlorophyll concentration; Karl and Lukas, 1996) with warm waters, whereas the waters of the Western Subarctic Gyre are cold and mesotrophic (Honda, 2003; Buesseler et al., 2008). Coccolithophorids ($CaCO_3$) are common off Hawaii (Cortes et al., 2001), whereas the waters of the Western Subarctic Gyre (e.g. stations K2 and K1; **Figure 1**) are dominated by diatoms (Honda et al., 2002; Honda et al., 2006). Station K3 also located in the northwestern North Pacific subarctic region is expected to be dominated by diatoms, based on sediment trap data from a nearby station (40°N/165°E) indicating that biogenic opal is predominant (Honda et al., 2002). The export of carbon is also higher in the Subarctic Gyre compared with the oligotrophic region off Hawaii (Buesseler et al., 2008).

The two investigated areas were studied later in the framework of the VERtical Transport In the Global Ocean, VERTIGO project, in years 2004 and 2005 (i.e., station Aloha, off Hawaii and station K2 in the Western Subarctic Gyre) (Buesseler et al., 2008). In particular, the Ba dataset (dissolved Ba and particulate Ba concentrations) obtained in the JPAC project on the entire water column can be compared to the Ba dataset collected during the VERTIGO project in the "twilight zone" (0-1000 m) (Dehairs et al., 2008). In addition, the vertical distribution of the ^{226}Ra activities reported here complement the study of Kawakami and Kusakabe (2008) who investigated the horizontal distribution of ^{226}Ra (and ^{228}Ra) in surface waters of the northwestern North Pacific Ocean. Time-series sediment trap moorings have been deployed in the northwestern North Pacific Ocean and provide information on sinking particle fluxes in the region (Honda, 2003).

The vertical profiles of potential temperature, salinity and potential density are reported in **Figure 2 of the Supplementary Material** for both stations K1 and K3. Station K3 is usually located north of the Kuroshio Front. However, Argo floats measurements conducted in the Northwest Pacific (Oka et al., 2015) indicate that the Kuroshio may sometimes extent toward station K3 (**Figure 3 of Supplementary Material**). This was the case in 2002, when station K3 was investigated in the present study, as indicated by the higher potential temperature and higher salinity in the upper 400 m at station K3 (**Figure 2 of Supplementary Material**) and by geochemical tracers (see *Ra Isotopic Ratios (^{228}Ra/^{226}Ra)*).

Sample Collection

Seawater samples were collected using 12 liter-Niskin bottles. Between 35 and 56 kg of seawater were collected at old station Hale Aloha and between 74 and 130 kg per depth were collected at stations K1 and K3 to a depth of 5200 m. Such relatively large seawater volumes were collected in order to allow the determination of ^{228}Ra - in addition to ^{226}Ra - which displays

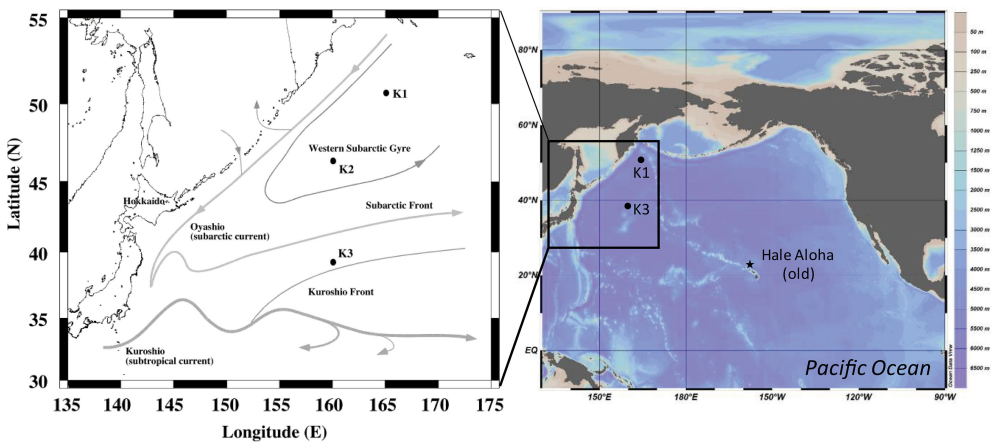

FIGURE 1 | Location of stations K1 and K3 investigated in the North-West Pacific. Station K2 investigated during the VERTIGO project is shown. Old station Hale Aloha, also investigated in this study, is located north of Hawaii Island, south of station ALOHA.

low concentrations in seawater. A separate aliquot (60 ml seawater) was collected for the determination of dissolved Ba concentrations. The large volume seawater samples (between 35 and 130 kg) were passed through a cartridge filled with acrylic fiber impregnated with MnO_2 (so called "Mn fibers"), following the technique described by Moore and Reid (1973). We used a flow-rate of 200 ml min^{-1} to ensure the quantitative separation of ^{226}Ra from seawater (Moore et al., 1985; van Beek et al., 2010).

Suspended particles were collected using McLane large volume pumps (WTS, McLane Labs, Falmouth, Ma, USA). Large volumes of seawater were filtered *in situ* through 142-mm diameter Versapor filters (acrylic copolymer on a nylon substrate; Pall Corporation), with a pore size of 0.8 µm. These large volume samples were required for gamma spectrometry and ICP-MS analyses. Additionally, seawater samples (9-11 L) were collected at station K3 using Niskin bottles and were passed through 47-mm polycarbonate filters with a pore size of 0.8 µm. To investigate the different Ba carriers within the suspended particles, the filters were sequentially leached using i, MilliQ water; ii, 10% (v/v) HNO_3; iii, 3% HCl; iv, hot 50% (v/v) HNO_3, following Ganeshram et al. (2003), slightly modified. Steps 1 to 3 were conducted on the ship immediately after collection using the clean room facility on RV Mirai. Step 4 was conducted back in the laboratory at the Woods Hole Oceanographic Institution (WHOI). Step 1 (MilliQ water) rinses dissolved Ba associated with residual seawater, weakly sorbed Ba and Ba released by cell lysis. 10% (v/v) nitric acid removes readily exchangeable and easily hydrolysable organically bound Ba. Celestite skeletons of acantharians, metal hydroxides and potentially also extracellular polymeric substances (EPS) are expected to be dissolved during steps 1 and 2. Step 3 - slightly modified from Ganeshram et al. (2003) following Weast et al. (1966), as done in van Beek and Reyss (2001) - dissolves $BaSO_4$. Finally, step 4 removes Ba associated with refractory organic matter.

Analytical Methods

For dissolved ^{226}Ra, the Mn fibers were ashed in a furnace for 16 hours at 820°C (Charette et al., 2001). The ash was then transferred into counting vials, sealed to prevent any Rn loss and analyzed for their radium activity using the low-background gamma spectrometers at the underground laboratory of Modane (Laboratoire Souterrain de Modane, LSM, French Alps) and at the underground laboratory of Ferrières (LAboratoire de mesure des FAibles RAdioactivités, LAFARA, French Pyrénées). High-efficiency, low-background, well-type germanium detectors (430 cm^3 and 950 cm^3 at LSM, Reyss et al., 1995; 280 cm^3 at LAFARA, van Beek et al., 2010; van Beek et al., 2013) were used. ^{226}Ra activities were determined using the ^{214}Pb (295 keV and 352 keV) and ^{214}Bi (609 keV) peaks. ^{228}Ra activities were determined using the 338, 911 and 969 keV peaks of ^{228}Ac. Counting times for each sample ranged from 2 to 5 days, in order to allow the detection of the low ^{228}Ra activities in addition to ^{226}Ra activities. Uncertainties for ^{226}Ra activities are errors due to counting statistics. The low counting background afforded by the counting facilities, the large sample volumes and the long counting times resulted in uncertainties for ^{226}Ra (ie. ± 1 to ± 3%) smaller than reported from most of the measurements performed during the GEOSECS program (± 3% to ± 10%).

For dissolved Ba, aliquots of seawater were analysed by isotope dilution using ^{135}Ba. The determination of dissolved Ba concentrations at old station Hale Aloha was conducted using the ICP-MS facility (Element, Finnigan) at WHOI. For samples collected in the North West Pacific (K1 and K3 stations), analyses were made using the ICP-MS facility at Scottish Universities Research and Reactor Centre, East Kilbride, Scotland (VG PlasmaQuad II). Uncertainty on the Ba concentrations is estimated at ± 2%.

For particulate ^{226}Ra and Ba, the filters were first placed in a counting tube and sealed prior to analysis to prevent any Rn loss, and counted for Ra isotopes using the low background gamma spectrometers at the underground laboratory of Modane (Laboratoire Souterrain de Modane, LSM, French Alps) using the same method as for dissolved ^{226}Ra. The Versapor filters were subsequently dissolved in a Teflon beaker with a mixture of HNO_3 (ultrapure acid), HF (ultrapure acid), and $HClO_4$ (pure acid) on a hot plate to measure Ba, ^{238}U and ^{232}Th using the ICP-MS facility at Observatoire Midi Pyrénées, Toulouse (Elan 6000 Perkin-Elmer), as described in van Beek et al. (2009). Excess Ba (Ba_{ex}), excess ^{226}Ra activities ($^{226}Ra_{ex}$) and excess ^{228}Ra activities ($^{228}Ra_{ex}$) in suspended particles were determined by subtracting the Ba, ^{226}Ra, and ^{228}Ra associated with the lithogenic component, as described in van Beek et al. (2007). The solutions obtained during sequential leaching were analyzed using the ICP-MS facility (Element, Finnigan) at WHOI.

Calculation of the Barite Saturation Index

The barite saturation index is defined as the ratio of the aqueous barium sulfate ionic product to the barite solubility product at a given temperature and pressure. For a given seawater sample, the concentrations of Na, K, Ca, Mg, Cl and SO_4 are calculated from the measured salinity and from the ionic composition of standard seawater (Millero, 2006). The measured Ba and Sr concentrations are then used along with the major element concentrations to calculate ionic activities in the Na-K-Ca-Mg-Ba-Sr-Cl-SO_4-H_2O system based on Pitzer's ion interaction model (Monnin and Galinier, 1988; Monnin, 1999), for the temperature and pressure of the sample under consideration. Sr substitution in barite has a limited influence on the barite saturation index (Monnin and Cividini, 2006).

RESULTS

Radium and Barium in Seawater

The ^{226}Ra activities and Ba concentrations determined in seawater at old station Hale Aloha, station K1, and station K3 are reported in **Tables 1-3 of the Supplementary Material**, and the vertical profiles are shown on **Figure 2**. Both increase with depth, reflecting uptake during particle formation in shallow waters and subsequent release at depth. Similar profiles were reported in the North Pacific during the GEOSECS program (Chung, 1976; Chung and Craig, 1980). The ^{226}Ra and Ba profiles

are similar at the three stations, but above 3000 m, Ba concentrations (and ^{226}Ra) are higher in the Subarctic Gyre (station K1) than at station K3 (**Figure 2**), while below 3000 m, there is a clear decrease in Ba concentrations at K1. The Ba concentrations at old station Hale Aloha are similar in June (lower sampling resolution) and August 2002 (**Table 1 of the Supplementary Material**). In the upper water column, the ^{226}Ra and Ba concentrations at station K1 are higher than those at stations located further south (K3 and old Hale Aloha), a pattern that was also observed during previous projects (Dehairs et al., 2008; Kawakami and Kusakabe, 2008). The higher concentrations in the upper waters of the northwestern North Pacific subarctic region are likely explained by the impact of the continents and continental margins in these regions (eg., Amakawa et al., 2004; Hawakami and Kusakabe, 2008; Lam and Bishop, 2008).

Barite Saturation Index

The barite saturation index was calculated at stations K1 and K3 considering either pure $BaSO_4$ or $(Ba,Sr)SO_4$ (**Figure 3**). The surface waters at K1 and K3 are undersaturated with respect to barite. Equilibrium is reached at approximately 500 m depth at station K1 and at approximately 1000 m depth at station K3. Below these depths, the waters are either in equilibrium or supersaturated with respect to barite down to approximately 3500 m at station K1 and down to approximately 5000 m at station K3. This pattern is characteristic of Pacific waters and agrees with that reported by previous studies (Monnin et al., 1999; Monnin and Cividini, 2006). This index can be used to provide information on the fate of barite within the water column (preservation *versus* dissolution), which may in turn impact the distributions of ^{226}Ra and Ba in the water column. Our data agree with those obtained at station K2 in the Western Subarctic Gyre and station Aloha off Hawaii by Dehairs et al. (2008) during the VERTIGO project.

^{226}Ra/Ba Ratio in Seawater

The Ba and ^{226}Ra concentrations are broadly consistent with the GEOSECS data set (Broecker et al., 1967; Wolgemuth and Broecker, 1970; Broecker et al., 1976; Chan et al., 1976; Chan et al., 1977; Moore et al., 1985). The ^{226}Ra/Ba ratios below 500 m agree with the GEOSECS value of 2.3 dpm μmol^{-1}. In contrast to many GEOSECS profiles, however, the data reported here display significantly lower ^{226}Ra/Ba ratios in the upper 500 m at stations K1, K3 and old station Hale Aloha (**Figure 4**). Near the seafloor, a decrease in the ^{226}Ra/Ba ratio is also observed at stations K1 and K3.

Barium and Radium in Suspended Particles

Some studies have reported Ra activities determined either in suspended particles (van Beek et al., 2007; van Beek et al., 2009;

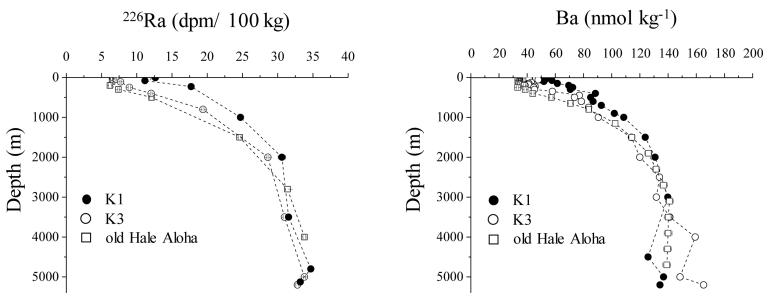

FIGURE 2 | Left panel: vertical profiles of ^{226}Ra at stations old Hale Aloha, K1 and K3 in the North Pacific. Right panel: vertical profiles of dissolved Ba at stations old Hale Aloha (August 2002 data), K1 and K3 in the North Pacific.

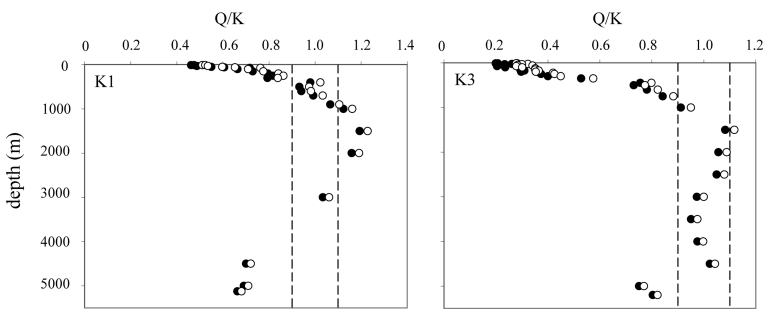

FIGURE 3 | Barite saturation index profiles at stations K1 and K3, considering either pure barite, $BaSO_4$ (black circles) or $(Ba,Sr)SO_4$ (open circles) in the calculations. Undersaturation is indicated by a saturation index lower than 1.0.

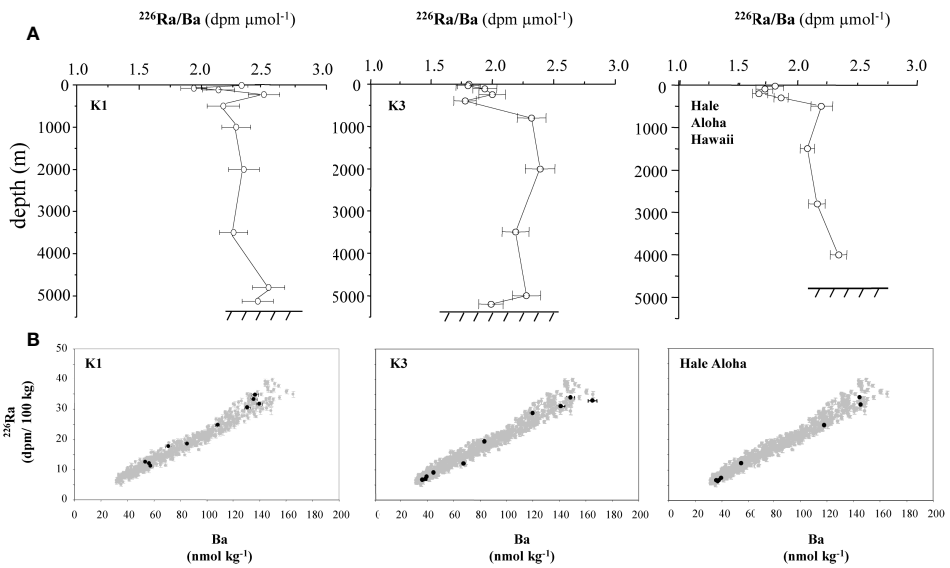

FIGURE 4 | Vertical profiles of ^{226}Ra/Ba ratios in seawater at the three investigated sites: stations K1 and K3 in the North West Pacific; old station Hale Aloha, off Hawaii **(A)**. The relationship between Ba and ^{226}Ra found at these stations (solid circles) is also compared to the Ba-^{226}Ra relationship reported from the GEOSECS program **(B)**.

Bourquin et al., 2011; van Beek et al., 2013) or in sinking particles collected with sediment traps (Moore and Dymond, 1991; Legeleux and Reyss, 1996; van Beek et al., 2007; van Beek et al., 2009) in the ocean. The vertical profiles of excess Ba concentrations (Ba_{ex}) and excess ^{226}Ra activities ($^{226}Ra_{ex}$) in suspended particles at stations K1 and K3 display maximum values between 200 and 500 m (**Figure 5**), similar to other oceanic basins (Dehairs et al., 1980; Dehairs et al., 1990; Jacquet et al., 2007; van Beek et al., 2007; Dehairs et al., 2008; Jacquet et al., 2008; van Beek et al., 2009). The Ba_{ex} and $^{226}Ra_{ex}$ vertical profiles at station K1 are remarkably similar, with both profiles displaying a double peak in the upper 400 m. For old station Hale Aloha, we report total ^{226}Ra activities that have not been corrected for lithogenic ^{226}Ra, though this correction is generally quite small (**Table 4 of the Supplementary Material**). The ^{226}Ra activities that have been determined at that station in June and August 2002 agree well with each other and display a maximum value at 250 m, a pattern that is also observed at station K1 (maximum ^{226}Ra activity at 230 m). The ^{226}Ra activities in suspended particles are lower at old station Hale Aloha than at stations K1 and K3 (**Figure 5**). The Ba_{ex} data that we report here for stations K1 and K3 agree with the values reported by Dehairs et al. (2008) at station K2 in the Western Subarctic Gyre during the VERTIGO project, with maximum values being approximately 500 pmol kg^{-1} in the upper 500 m. Dehairs et al. (2008) report Ba_{ex} concentrations that were lower at station

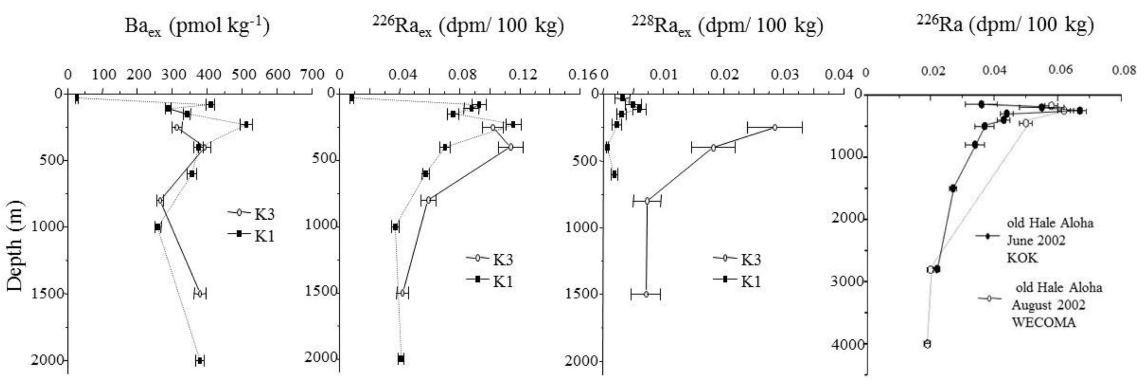

FIGURE 5 | Vertical profiles of excess Ba (Ba_{ex}) concentrations, excess ^{226}Ra ($^{226}Ra_{ex}$) activities and excess ^{228}Ra ($^{228}Ra_{ex}$) determined in suspended particles collected at stations K1 and K3. We also report the ^{226}Ra activities (not corrected for the supported ^{226}Ra) determined in the suspended particles collected at old station Hale Aloha in June and August 2002.

Aloha than at station K2, a pattern that is similar for the $^{226}Ra_{ex}$ activities reported here. We also report $^{228}Ra_{ex}$ activities determined at stations K1 and K3 (**Figure 5**). The $^{228}Ra_{ex}$ activities are higher in the upper 500 m of the water column, a pattern that was also observed in other oceanic basins (van Beek et al., 2007; van Beek et al., 2009). We will later compare the $^{228}Ra/^{226}Ra$ ratios of the suspended particles to the dissolved $^{228}Ra/^{226}Ra$ ratios (see *Ra Isotopic Ratios ($^{228}Ra/^{226}Ra$)*).

DISCUSSION

The phases that are believed to incorporate or adsorb Ba (and Ra) in the water column are i) barite, ii) celestite produced by acantharians (Dehairs et al., 1980; Bernstein et al., 1992), iii) extracellular polymeric substances (EPS; Martinez-Ruiz et al., 2020), iv) Fe hydroxides (Sternberg et al., 2005), v) diatoms or metal hydroxides attached to diatoms (Bishop, 1988; Ganeshram et al., 2003; Sternberg et al., 2005), vi) calcareous skeletons (Lea and Boyle, 1989), with barite being often cited as the main Ba (and Ra) carrier in the water column (Dehairs et al., 1980; Moore and Dymond, 1991; Legeleux and Reyss, 1996; Martinez-Ruiz et al., 2020). Since the world's oceans are mostly undersaturated with respect to barite (Church and Wolgemuth, 1972; Monnin et al., 1999; Rushdi et al., 2000; Monnin and Cividini, 2006), it was proposed that barite precipitation takes place in the upper water column within supersaturated microenvironments of decaying organic matter (Chow and Goldberg, 1960; Dehairs et al., 1980; Bishop, 1988; Dehairs et al., 1990; Dehairs et al., 1991; Dehairs et al., 1992; Ganeshram et al., 2003). In the North Pacific, the waters are undersaturated with respect to barite in the upper 500 m (K1) and 1000 m (K3) (**Figure 3**) and in the upper 1000 m at station ALOHA (Dehairs et al., 2008). The Ba_{ex} and $^{226}Ra_{ex}$ maxima observed in suspended particles in the upper 500 m are thus located within undersaturated waters, further suggesting that barite forms within microenvironments. Besides barite, acantharian celestite, EPS or Fe hydroxides may contribute significantly to Ba_{ex} and $^{226}Ra_{ex}$. Because acantharians are mostly found in the upper 150 m (Bishop et al., 1977; Bishop et al., 1978; Michaels, 1988; Bernstein et al., 1992; Michaels et al., 1995), their contribution must be restricted to shallow water.

^{226}Ra/Ba Ratio in Suspended Particles

The ^{226}Ra/Ba ratios in suspended particles are higher in the upper water column and decrease with increasing water depth (**Figure 6**). Two samples collected at station K3 in the upper 500 m display ^{226}Ra/Ba ratios that are higher than the 2.3 dpm μmol^{-1} (i.e. 3.2±0.3 dpm μmol^{-1} at 250 m and 2.9±0.3 dpm μmol^{-1} at 400 m). At station K1, two samples collected in waters above 150 m display high ratios (3.0 dpm μmol^{-1} at 30 m and 110 m), but ratios close to 2.3 dpm μmol^{-1} were also found at 80 m, 150 m and 230 m, indicating spatial heterogeneity in the composition/origin of the suspended particles.

Below 400-500 m, the ^{226}Ra/Ba ratios in suspended particles are equal to or lower than the 2.3 dpm μmol^{-1} value. Similar patterns were found in other oceanic basins (van Beek et al., 2007; van Beek et al., 2009). The higher ^{226}Ra/Ba ratios found in suspended particles compared to the ratio in seawater at the same depth indicates that fractionation between ^{226}Ra and Ba takes place during formation of suspended particles in the water column, contrary to earlier assumptions (Wolgemuth and Broecker, 1970; Ku and Luo, 1994).

Ba Carriers at Station K3

The sequential leaching method of Ganeshram et al. (2003) was applied to an entire vertical profile of suspended particles collected with Niskin bottles (station K3) in order to provide additional information on the different Ba carriers within the water column (**Table 1**). In surface waters down to 110 m, Ba is mostly found in the fractions released by the first two leaching steps (MilliQ water and 10% HNO_3), which suggests that the Ba pool in surface waters down to 110 m is relatively labile (**Figure 7**). The labile pool of Ba at these depths likely consists in i) labile organic matter, including potentially EPS, ii) acantharians that are generally concentrated in surface waters (Michaels, 1988; Michaels et al., 1995) and iii) oxy-hydroxides. This labile pool of Ba then decreases with increasing water depth

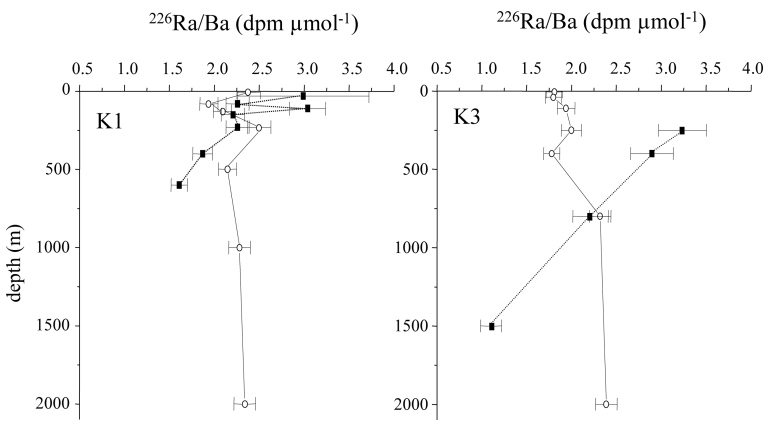

FIGURE 6 | Vertical profiles of ^{226}Ra/Ba ratios determined at stations K1 and K3 in suspended particles (black squares) and in seawater (open circles).

TABLE 1 | Ba concentrations (pmol kg^{-1}) determined in the different particulate fractions at station K3 using the sequential leaching method of Ganeshram et al. (2003), slightly modified.

Depth (m)	Ba (pmol kg $^{-1}$) ± 2%	%	Ba (pmol kg $^{-1}$) ± 2%	%	Ba (pmol kg $^{-1}$) ± 2%	%	Ba (pmol kg $^{-1}$) ± 2%	%	Sr (pmol kg $^{-1}$) ± 3%	Sr/Ba (mol/mol) ± 7%
	Fraction #1 ***Labile matter*** **(MilliQ water)**		**Fraction #2** ***Labile matter*** **(10% HNO_3)**		**Fraction #3** ***$BaSO_4$*** **(3% HCl)**		**Fraction #4** ***Refractory OM*** **(hot HNO_3)**		**Fraction #3** ***$BaSO_4$*** **(3% HCl)**	**Fraction #3** ***$BaSO_4$*** **(3% HCl)**
40	122	12.2	406	40.8	194	19.5	274	27.5	199	1.026
110	52	8.6	311	51.2	205	33.8	39	6.4	265	1.293
250	24	1.1	174	8.2	1680	79.1	245	11.5	38	0.023
400	32	4.7	144	21.2	445	65.5	58	8.5	_	_
800	29	3.6	244	30	403	49.3	136	16.7	14	0.035
2000	55	5.9	177	18.9	629	67.1	76	8.1	12	0.019
3500	29	6.4	91	23.0	236	59.6	40	10.1	20	0.085
5000	20	7.0	85	29.8	166	58.2	14	4.9	11	0.066

The Sr concentration (pmol kg^{-1}) and the Sr/Ba (mol/mol) determined in fraction #3 (assumed to be $BaSO_4$) are also reported. The relative contribution of each fraction is also reported (%).

such that below 200 m, barite appears to be the dominant Ba carrier. This pattern thus agrees with the view that the decrease in the labile pool of Ba - following the decay of organic matter or dissolution of acantharian celestite - provides Ba in the microenvironment for barite precipitation in subsurface water (Chow and Goldberg, 1960; Dehairs et al., 1980; Legeleux and Reyss, 1996; Ganeshram et al., 2003; Sternberg et al., 2005; Martinez-Ruiz et al., 2020). The Ba_{ex} concentrations (non lithogenic Ba) are often considered to reflect barite, although Ba_{ex} may also include Ba associated with the different fractions invoked above; these latter Ba carriers can be considered as relatively minor contributors below 110 m (**Table 1**). The Ba_{ex} concentrations determined in suspended particles collected using *in situ* pumps below the surface down to 2000 m (250-550 pmol kg^{-1}; **Figure 5**) are in relatively good agreement with the Ba concentrations associated with $BaSO_4$ in fraction #3 (200-630 pmol kg^{-1}; **Figure 7**) over the same depth interval, with the exception of a sharp peak at 250 m found in the sequential leaching experiment (1680 pmol kg^{-1}). This discrepancy may reflect spatial variability that leads to slightly different samples collected by the two methods (Niskin bottles versus *in situ* pumps). Note that such high particulate Ba concentrations (1680 pmol kg^{-1}) have already been reported by previous studies in other oceanic regions (Jacquet et al., 2007; van Beek et al., 2009) and correspond to a depth where the rate of barite precipitation is believed to be highest (e.g., Legeleux and Reyss, 1996). Maximal Ba_{ex} and $^{226}Ra_{ex}$ concentrations were also found at this depth (**Figure 5**). The Ba concentration associated with $BaSO_4$ remains relatively high down to 2000 m (629 pmol kg^{-1}; **Figure 7**), a pattern that may be related to the saturation state of intermediate waters with respect to barite in the North Pacific that preserves barite or limits its dissolution while settling (**Figure 3**). At 5000 m, the Ba concentration associated with $BaSO_4$ is significantly lower than in the upper 500 m (166 pmol kg^{-1}), suggesting dissolution in water undersaturated with respect to barite. The pool of Ba associated with refractory

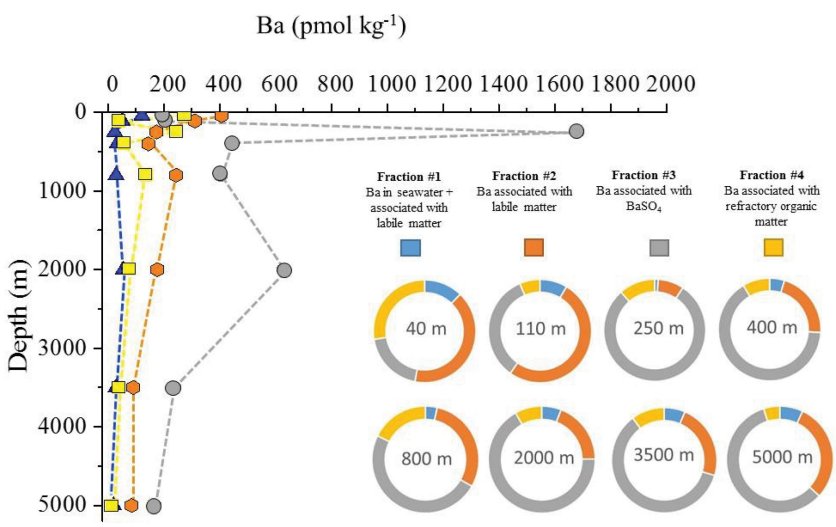

FIGURE 7 | Vertical profiles of Ba concentrations determined in the different particulate fractions collected using the sequential leaching method of Ganeshram et al. (2003) at station K3. The relative importance of the different fractions is also shown at each depth.

organic matter decreases from the surface to the bottom. While the sharp decrease in the labile Ba pool in the upper 500 m may be the main contributor to barite precipitation in the upper water column, the release of the Ba associated with refractory organic matter at depth may also contribute to barite precipitation in waters below 500 m (van Beek et al., 2007).

The Sr concentration and the Sr/Ba ratio was also investigated in fraction #3 that is associated to $BaSO_4$ (**Table 1**). High Sr concentrations and high Sr/Ba ratios (1.0-1.1 mol/mol) were found in samples collected in surface waters (40 m and 110 m). Since acantharian skeletons are expected to dissolve in the first two leaching steps, the high Sr concentrations found in fraction #3 are unlikely from acantharians, but must be included in $BaSO_4$. The high Sr content in these barite samples may indicate that barite found at these depths precipitated in microenvironments where significant dissolution of celestite took place and/or following a prior step of Sr-Ba bioaccumulation by EPS (since EPS was shown to concentrate Sr in addition to Ba; Martinez-Ruiz et al., 2020). Below 250 m, the Sr/Ba ratios are lower (0.019-0.085 mol/mol). These latter values are in good agreement with the ratios reported in barite separated from sediments collected in the Pacific Ocean (0.03-0.05 mol/mol; van Beek et al., 2003). This observation further supports the association of fraction #3 with $BaSO_4$. The different Sr/Ba ratios in $BaSO_4$ found either above or below 110 m may indicate a larger influence of the dissolution of acantharian skeletons - that releases Ba, Sr and Ra into the microenvironments - in barite formation in the upper 110 m or an evolution of the ratio following dissolution of barite during settling. Like the Sr/Ba ratio in fraction #3, the $^{226}Ra_{ex}$/Ba_{ex} ratio in suspended particles is also higher in the upper water column and decreases with increasing depth (**Figure 6**). This pattern is also observed in the Sr concentrations and Sr/Ba ratios determined in suspended particles collected with *in situ* pumps (**Table 4 of the Supplementary Material**). The latter Sr/Ba ratios being higher than the Sr/Ba ratio determined from the sequential leaching in fraction #3 may be explained by the different Sr and Ba contributors in these samples (i.e. residual seawater, carbonates, barite, celestite), which would serve to mask the Sr/Ba ratio in barite. Similar relationships were found in the upper 150 m between Ra, Sr and Ba at the OFP station in the Sargasso Sea and at the DYFAMED station in the western Mediterranean Sea: high ^{226}Ra/Ba ratios were found in both suspended and sinking particles with ratios being much higher than the ambient seawater ^{226}Ra/Ba ratios. Values up to 3.8 dpm μmol^{-1} were observed at 120 m in the Sargasso Sea (van Beek et al., 2007) and up to 8.4 dpm μmol^{-1} at 140 m in the western Mediterranean Sea (van Beek et al., 2009), at depths where acantharians are found. In these latter studies, the relationship with acantharians was further suggested by the high particulate Sr content determined in the suspended particles in the upper 150 m of the two regions (van Beek et al., 2007; van Beek et al., 2009) and by the observation of acantharian skeletons on filters collected in the western Mediterranean Sea (van Beek et al., 2009).

Ra Isotopic Ratios (^{228}Ra/^{226}Ra)

The vertical gradient of the dissolved ^{228}Ra/^{226}Ra ratio in the water column allows us to investigate the depth of particulate Ba formation in the water column (Legeleux and Reyss, 1996; van Beek et al., 2007; **Figure 8**). The much higher dissolved ^{228}Ra/^{226}Ra ratios in the upper 500 m at station K3 compared with station K1 are due to higher dissolved ^{228}Ra activities (**Figure 9**) resulting from the northward extension of the Kuroshio to station K3 in 2002 (Oka et al., 2015; **Figures 2** and **3 of Supplementary Material**). These waters acquired ^{228}Ra when interacting with the sediments of the continental shelf when they were flowing northeastward along Honshu (Kaufman et al., 1973; Kawakami and Kusakabe, 2008; Charette et al., 2013). Consequently, the $^{228}Ra_{ex}$ signature of the suspended particles is also higher at station K3 in comparison to station K1 (**Figure 5**). At station K1, the ^{228}Ra/^{226}Ra ratios in the suspended particles collected in the upper 500 m generally match the ^{228}Ra/^{226}Ra ratios in the dissolved phase (**Figure 8**): the ^{228}Ra/^{226}Ra ratios in the particulate phase in the upper 500 m follow the profile of the dissolved phase. This suggests that the particulate Ba collected at each of these depths was formed at these water depths and thus incorporated the ^{228}Ra/^{226}Ra signature of the dissolved phase. This observation agrees with previous studies conducted in other oceanic basins (van Beek et al., 2007; van Beek et al., 2009). At station K3, the ^{228}Ra/^{226}Ra ratios in the particulate phase in the upper 500 m are slightly higher than the dissolved phase, but

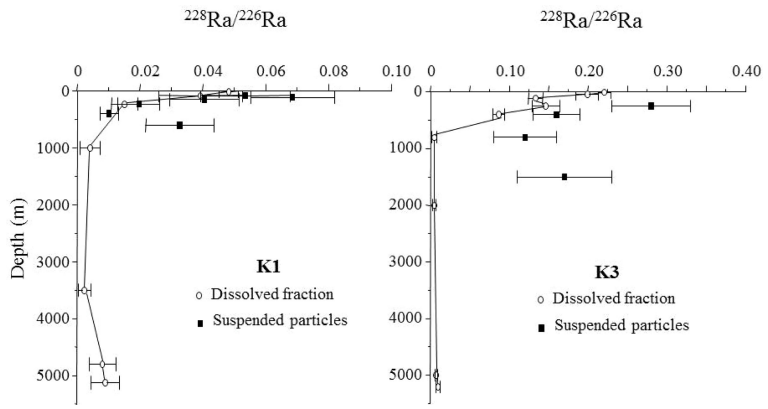

FIGURE 8 | Comparison of the ^{228}Ra/^{226}Ra ratios determined in the dissolved phases and suspended particles at stations K1 and K3.

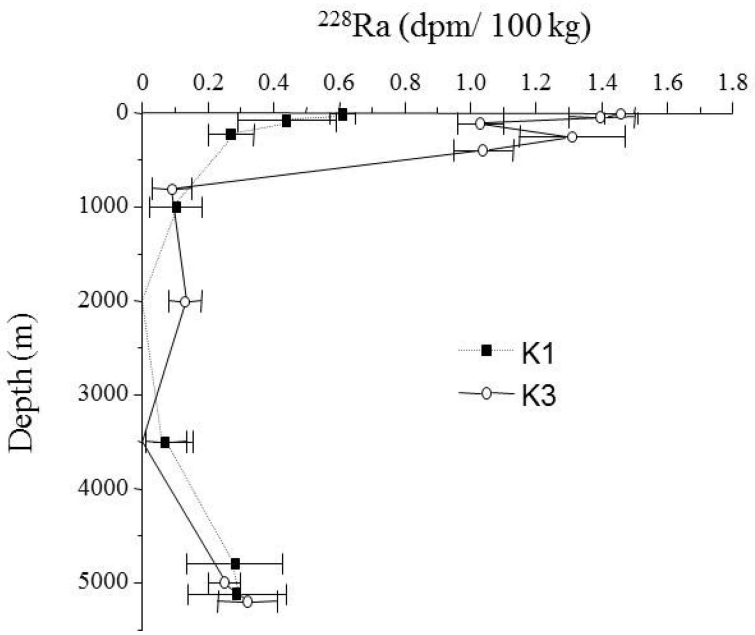

FIGURE 9 | Vertical profiles of dissolved ^{228}Ra activities determined at stations K1 and K3 in the North Pacific. The large difference in ^{228}Ra activities the upper 500 m between stations K1 and K3 is attributed to the extension of the Kurushio current that reached station K3 in year 2002 during the present study.

remain close to the seawater ratios. Like at station K1, this may suggest that the particles incorporated the ^{228}Ra/^{226}Ra signature of the dissolved phase at these depths.

Below 500 m, the ^{228}Ra/^{226}Ra ratios in the particulate phase are higher than the seawater ratios at the corresponding depth at both stations K1 and K3 suggesting that particulate Ba originates from shallower depths, where it acquired a higher ^{228}Ra/^{226}Ra ratio. At these depths, the particulate Ba is mostly associated with barite (**Figure 7**) that are found at depths where the waters are in equilibrium or supersaturated with respect to barite (**Figure 3**). This indicates that the particulate Ba at intermediate depths (500-1500 m) mostly consists of settling barite that was formed in the upper 500 m of the water column. Such high particulate ^{228}Ra/^{226}Ra ratios indicating an export of barite formed in shallower waters were previously observed in other oceanic basins but only in sinking particles collected with sediment traps (Legeleux and Reyss, 1996; van Beek et al., 2007; van Beek et al., 2009) and not in suspended particles (e.g. van Beek et al., 2007). The sharp decrease in the Ba concentration associated with barite (fraction #3) below the Ba peak at 250 m (**Figure 7**) - that indicates a maximum rate of barite formation at these depths - suggests that a large fraction of barite then dissolves in the upper 500 m of the water column (that were shown to be undersaturated with respect to barite) and are not exported to greater depth.

^{226}Ra-Ba Relationship

The general relationship between Ba and ^{226}Ra (**Figure 1 of Supplementary Material**) led Chan et al. (1976) to propose that there was a constant ratio between Ba and ^{226}Ra in the ocean above 2500 m (4.6 nmol ^{226}Ra/mol Ba, equivalent to 2.3 dpm μmol^{-1}). The data reported here indicate that ^{226}Ra/Ba ratios significantly lower than 2.3 dpm μmol^{-1} can be found in the upper 500 m of the water column. A similar trend was observed in the Sargasso Sea (Ocean Flux Program Time-Series; van Beek et al., 2007; **Figure 10**). van Beek et al. (2009) also reported low ^{226}Ra/Ba ratios (1.3-1.8 dpm μmol^{-1}) at the DYFAMED Time-Series in the Mediterranean Sea, but these low ratios were found throughout the water column (van Beek et al., 2009; **Figure 10**). Data from the Mediterranean Sea thus clearly fall below the regression obtained with the GEOSECS data (**Figure 10B**), a pattern that may - at least partly - be explained by the anti-estuarine circulation in the Mediterranean Sea that fills the entire basin with water originating from the upper water column of the Atlantic Ocean (expected to display a low ^{226}Ra/Ba ratio, following van Beek et al., 2007). The data from the Mediterranean Sea also clearly highlight the temporal variability of the ^{226}Ra/Ba ratio at the DYFAMED station.

Many of the vertical profiles obtained during GEOSECS do not show lower ^{226}Ra/Ba ratios in the upper water column. This could be attributed to the lower sampling resolution and precision of the GEOSECS Ba and ^{226}Ra measurements (Ku and Luo, 1994). We note however, that when all the ^{226}Ra/Ba profiles obtained during the GEOSECS program for each ocean basins are plotted versus depth, the lowest ^{226}Ra/Ba ratios are invariably found in the upper 500 m of the water column (left of the vertical line on **Figure 11**). Likewise, as noted before (Wolgemuth and Broecker, 1970; Chan et al., 1976; Ku and Luo, 1994), the linear regression of ^{226}Ra activity versus Ba concentration has a significant, positive intercept on the Ba

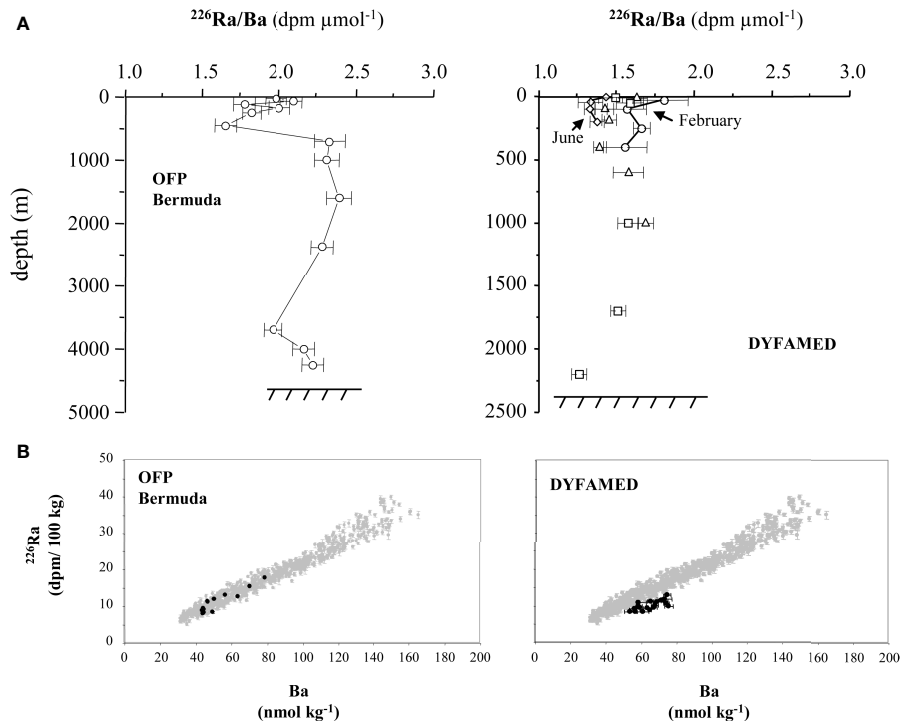

FIGURE 10 | Vertical profiles of ^{226}Ra/Ba ratios reported in seawater in other oceanic basins by previous studies: Sargasso Sea, Atlantic Ocean (van Beek et al., 2007) and Mediterranean Sea (van Beek et al., 2009) **(A)**. The relationship between Ba and ^{226}Ra found at these stations is also compared to the Ba-^{226}Ra relationship reported from the GEOSECS program **(B)**.

axis (**Figure 1 of the Supplementary Material**). The pattern reported here (i.e., low ^{226}Ra/Ba ratios in the upper 500 m) does not appear universal, however. In particular, data from Foster et al. (2004) and Staubwasser et al. (2004) indicate that surface waters in the Ross Sea have ^{226}Ra/Ba ratios similar to deep waters. This pattern is consistent with the deep convective mixing that dominates this region, which may mask fractionation observed in other regions. This is further confirmed by the lack of an intercept when regressing ^{226}Ra activity and Ba concentration measured in samples from the Southern Ocean (Li et al., 1973).

Processes Affecting the ^{226}Ra/Ba Ratios

The intercept on the regression of ^{226}Ra activity versus Ba concentration has been attributed to the differences in the source of the two elements (Wolgemuth and Broecker, 1970; Chan et al., 1976; Ku and Luo, 1994). While Ba is mainly added to the upper ocean by rivers and potentially also by SGD, ^{226}Ra is mostly added to the ocean by diffusion from deep-sea sediments. Simple two box models show that such differences in input can generate a lower ^{226}Ra/Ba in the upper water column (Chan et al., 1976). However, the difference in the ratio produced by these simple models is smaller than those observed in the measurements reported here, suggesting that other mechanisms contribute to the observed vertical changes in Ra/Ba.

Barite, celestite, EPS and hydroxides (e.g. Fe, Mn hydroxides) are known to incorporate or adsorb Ba and Ra. Barite and celestite are believed to be the main Ba carriers in the water column, and to explain the vertical profiles of particulate Ba_{ex} and $^{226}Ra_{ex}$, which have higher concentrations in the upper ca. 500 m. The two main Ba (and Ra) carriers are not found at exactly the same water depth: the presence of celestite is mostly restricted to the upper 150 m, whereas barite is usually found below that depth (maximum concentration often observed at ca. 200-250 m). The high ^{226}Ra/Ba ratios in suspended particles reported in this study were found both at shallow depths dominated by acantharians, as deduced from elevated particulate Sr concentrations (30 m and 110 m, station K1) and barite (250 m and 400 m, station K3). Because celestite is expected to be enriched in radium compared to barium (Bernstein et al., 1998), the high ^{226}Ra/Ba ratios found in suspended particles in the upper ca. 150 m may be attributed to acantharian skeletons; such a fractionation process may thus contribute to decrease the dissolved ^{226}Ra/Ba ratios in the upper water column. As deduced from the leaching experiments, barite (fraction #3) formed in the upper 110 m displays high Sr/Ba ratios, suggesting a potential link between acantharian skeletons and barite formation at these depths. The high ^{226}Ra/Ba ratios found

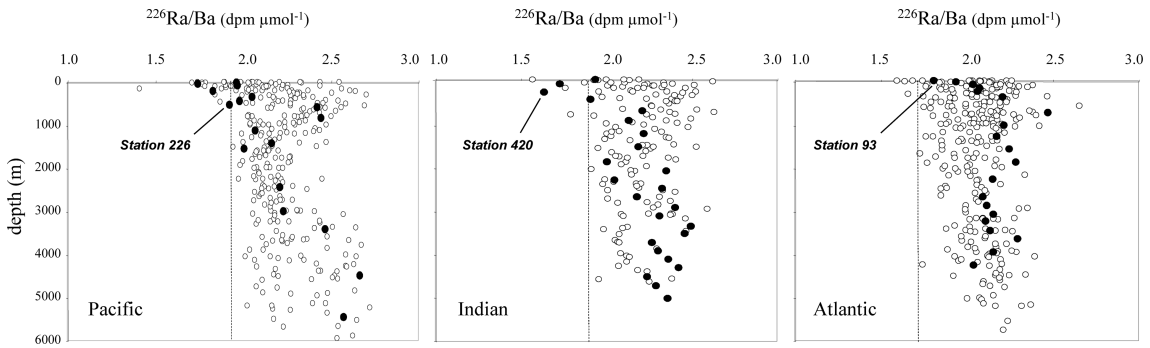

FIGURE 11 | Compilation of the vertical distributions of ^{226}Ra/Ba ratios reported in the Pacific, Indian and Atlantic Oceans during the GEOSECS program (open circles). Ratios found at station #226 (Pacific Ocean), station #420 (Indian Ocean) and station #93 (Atlantic Ocean) are underlined on the graphs (closed circles). The vertical line is placed to highlight the lower ^{226}Ra/Ba ratios found in the upper water column (left of the line) at several stations.

in the suspended particles at shallow depths may thus be related to celestite and to barite precipitating in microenvironments in which celestite - with a high ^{226}Ra/Ba ratio - rapidly dissolves (Bernstein et al., 1987; Bernstein et al., 1992). Deeper in the water column, the leaching experiments showed that the decrease in the labile pool of Ba down to ca. 250 m (e.g. decay of labile organic matter) was accompanied by increased barite formation. Fractionation between Ba and Ra may thus take place during the bioaccumulation phase of Ba-Ra prior to barite formation within the microenvironments (e.g. adsorption onto bacterial biofilms; Martinez-Ruiz et al., 2020) or during barite precipitation itself. Below 500 m, the ^{226}Ra/Ba ratios in suspended particles are lower than the ambient seawater ^{226}Ra/Ba ratios in the three studies that have investigated both particulate and dissolved Ba and Ra (van Beek et al., 2007; van Beek et al., 2009; this study). The ^{226}Ra/Ba ratios may thus be impacted during dissolution of barite that settles in undersaturated waters.

CONCLUSION

Seawater ^{226}Ra/Ba ratios close to 2.3 dpm µmol^{-1} were found below 500 m at three sites in the North Pacific Ocean, in agreement with ratios reported during the GEOSECS program. In contrast, we report significantly lower ^{226}Ra/Ba ratios in the upper 500 m of the water column. This pattern is similar to that observed in other areas of the world's ocean, such as the Sargasso Sea (van Beek et al., 2007) and the western Mediterranean Sea (van Beek et al., 2009). While this trend may partly be attributed to differences in the source of these two elements, other processes must be contributing to the contrast between the ^{226}Ra/Ba ratio of surface and deep waters. The ^{226}Ra/Ba ratio in suspended particles indicates that fractionation between Ba and ^{226}Ra takes place in the upper ca. 500 m of the water column.

Our results suggest that ^{226}Ra enrichment relative to Ba in celestite and mass fractionation during barite formation (or during a precursor stage of barite formation, i.e. when Ba and Ra accumulate within the microenvironments, involving potentially bacterial biofilms as proposed by Martinez-Ruiz et al., 2020) may lead to such fractionation between Ba and Ra in the upper 500 m. The spatial and seasonal variability of upper ocean ^{226}Ra/Ba ratios and fractionation between Ba and Ra have implications for the use of ^{226}Ra as a dating tool or as a tracer of abyssal circulation and mixing, which rely on a lack of fractionation between the two elements during biological cycling (Ku and Luo, 1994). This assumption now appears to be violated for large regions of the ocean. In addition, dating methods based on the decay of ^{226}Ra require that the initial ^{226}Ra/Ba be known and constant. For example, previous studies have assumed that the initial ratio was the mean value obtained from GEOSECS (i.e., 2.3 dpm µmol^{-1}). While this assumption may be valid for Antarctic samples (Staubwasser et al., 2004), it might not be the case for most other oceanic regions, if the sample to be dated has been formed in shallow waters.

DATA AVAILABILITY STATEMENT

The original contributions presented in the study are included in the article/**Supplementary Material**. Further inquiries can be directed to the corresponding author.

AUTHOR CONTRIBUTIONS

PB, RF, MH, and SH designed and coordinated the different studies. PB performed the sampling, analyses and provided the datasets. J-LR contributed to the analyses. CM provided the barite saturation index. PB, RF, MH, MC, RG, and CM contributed to the interpretation of data. PB wrote the first draft of the manuscript and all authors contributed to the final version of the manuscript.

ACKNOWLEDGMENTS

We are grateful to the crews and captains of RV WECOMA (USA), RV Ka'imikai-o-Kanaloa (USA) and RV Mirai (Japan). We thank Mike Bacon, chief scientists on board RV WECOMA and RV KoK. We thank Kazuhiro Hayashi and Markus Kienast for their help during sampling on board RV Mirai. We thank Larry Ball and David Schneider at the ICP/MS of WHOI, USA, and Valérie Olive at the ICP/MS of East Kilbride, Scotland, UK. We also thank Alan Fleer and Susan Brown-Léger at WHOI for their help in the lab and at sea (Hale Aloha). We thank Charlotte Riccio, Thierry Sampieri and Jean-Louis Saury at the underground laboratory of Modane (LSM). We thank Rémi Freydier and Marc Souhaut for their help at the ICP/MS at Observatoire Midi Pyrénées. We thank Steven Manganini and Jerzy Blusztajn for constructive discussions on the project. This work was supported by a Lavoisier fellowship attributed by the French Ministry of Foreign Affairs to PB in year 2002 and by the Woods Hole Oceanographic Institution (WHOI). This work was completed at the University of Edinburgh in 2003, while PB was a postdoctoral fellow there, with a Marie Curie fellowship from the European Union. The European Union is thus also thanked. MC acknowledges support from the National Science Foundation, Chemical Oceanography program. We thank the two reviewers for their constructive comments that allowed us to improve the quality of the manuscript, as well as Nuria Casacuberta and Paul MacGinnity, associate editors. This paper is dedicated to the memory of SH.

PB and Markus Kienast are sampling Niskin bottles on board RV Mirai in the NW Pacific under the supervision of Susumu Honjo (December 2002).

SUPPLEMENTARY MATERIAL

The Supplementary Material for this article can be found online at: https://www.frontiersin.org/articles/10.3389/fmars.2022.859117/full#supplementary-material

REFERENCES

Amakawa, H., Nozaki, Y., Sotto Alibo, D., Zhang, J., Fukugawa, K., and Nagai, H. (2004). Neodymium Isotopic Variations in Northwest Pacific Waters. *Geochim. Cosmochim. Acta* 68, 715–727. doi: 10.1016/S0016-7037(03)00501-5

Bacon, M. P., and Edmond, J. M. (1972). Barium at GEOSECS III in the Southwest Pacific. *Earth Planet Sci. Lett.* 16, 66–74. doi: 10.1016/0012-821X(72)90237-3

Berkman, P. A., and Ku, T.-L. (1998). ^{226}Ra/Ba Ratios for Dating Holocene Biogenic Carbonates in the Southern Ocean : Preliminary Evidence From Antarctic Coastal Mollusc Shells. *Chem. Geol.* 144, 331–334. doi: 10.1016/S0009-2541(97)00137-X

Bernstein, R. E., Betzer, P. R., Feely, R. A., Byrne, R. H., Lamb, M. F., and Michaels, A. F. (1987). Acantharian Fluxes and Strontium to Chlorinity Ratios in the North Pacific Ocean. *Science* 237, 1490–1494. doi: 10.1126/science.237.4821.1490

Bernstein, R. E., and Byrne, R. H. (2004). Acantharians and Marine Barite. *Mar. Chem.* 86, 45–50. doi: 10.1016/j.marchem.2003.12.003

Bernstein, R. E., Byrne, R. H., Betzer, P. R., and Greco, A. M. (1992). Morphologies and Transformations of Celestite in Seawater: The Role of Acantharians in Strontium and Barium Geochemistry. *Geochim. Cosmochim. Acta* 56, 3273–3279. doi: 10.1016/0016-7037(92)90304-2

Bernstein, R. E., Byrne, R. H., and Schijf, J. (1998). Acantharians: A Missing Link in the Oceanic Biogeochemistry of Barium. *Deep-Sea Res. II* 45, 491–505. doi: 10.1016/S0967-0637(97)00095-2

Bishop, J. K. B. (1988). The Barite-Opal-Organic Carbon Association in Oceanic Particulate Matter. *Nature* 332, 341–343. doi: 10.1038/332341a0

Bishop, J. K. B., Edmond, J. M., Ketten, D. R., Bacon, M. P., and Silker, W. B. (1977). The Chemistry, Biology, and Vertical Flux of Particulate Matter From the Upper 400 M of the Equatorial Atlantic Ocean. *Deep-Sea Res.* 24, 511–548. doi: 10.1016/0146-6291(77)90526-4

Bishop, J. K. B., Ketten, D. R., and Edmond, J. M. (1978). The Chemistry, Biology, and Vertical Flux of Particulate Matter From the Upper 400 M of the Cape Basin in the Southeast Atlantic Ocean. *Deep-Sea Res.* 25, 1121–1161. doi: 10.1016/0146-6291(78)90010-3

Bourquin, M., van Beek, P., Reyss, J. L., Riotte, J., and Freydier, R. (2011). Determination of ^{226}Ra Concentrations in Seawater and Suspended Particles (NW Pacific) Using MC-ICP-MS. *Mar. Chem.* 126, 132-138. doi: 10.1016/j.marchem.2011.05.001

Broecker, W. S., Goddard, J., and Sarmiento, J. L. (1976). The Distribution of ^{226}Ra in the Atlantic Ocean. *Earth Planet Sci. Lett.* 32, 220–235. doi: 10.1016/0012-821X(76)90063-7

Broecker, W. S., Li, Y. H., and Cromwell, J. (1967). Radium-226 and Radon-222: Concentration in Atlantic and Pacific Oceans. *Science* 158, 1307–1310. doi: 10.1126/science.158.3806.1307

Buesseler, K.O., Trull, T.W., Steinberg, D.K., Silver, M.W., Siegel, D.A., Saitoh, S.-I., et al. (2008). VERTIGO (VERtical Transport In the Global Ocean): A Study of Particle Sources and Flux Attenuation in the North Pacific. *Deep-Sea Res. II* 55, 1522–1539. doi: 10.1016/j.dsr2.2008.04.024

Chan, L. H., Drummond, D., Edmond, J. M., and Grant, B. (1977). On the Barium Data From the Atlantic GEOSECS Expedition. *Deep-Sea Res.* 24, 613–649. doi: 10.1016/0146-6291(77)90505-7

Chan, L. H., Edmond, J. M., Stallard, R. F., Broecker, W. S., Chung, Y. C., Weiss, R. F., et al. (1976). Radium and Barium at GEOSECS Stations in the Atlantic and Pacific. *Earth Planet Sci. Lett.* 32, 258–267. doi: 10.1016/0012-821X(76)90066-2

Charette, M. A., Breier, C. F., Henderson, P. B., Pike, S. M., Rypina, I. I., Jayne, S. R., et al. (2013). Radium-Based Estimates of Cesium Isotope Transport and Total Direct Ocean Discharges From the Fukushima Nuclear Power Plant Accident. *Biogeosciences* 10, 2159–2167. doi: 10.5194/bg-10-2159-2013

Charette, M. A., Buesseler, K. O., and Andrews, J. E. (2001). Utility of Radium Isotopes for Evaluating the Input and Transport of Groundwater-Derived Nitrogen to a Cape Cod Estuary. *Limnol. Oceanogr.* 46 (2), 465–470. doi: 10.4319/lo.2001.46.2.0465

Chow, T. J., and Goldberg, E. D. (1960). On the Marine Geochemistry of Barium. *Geochim. Cosmochim. Acta* 20, 192–198. doi: 10.1016/0016-7037(60)90073-9

Chung, Y.-C. (1974). Radium-226 and Ra-Ba Relationships in Antarctic and Pacific Waters. *Earth Planet Sci. Lett.* 23, 125–135. doi: 10.1016/0012-821X(74)90039-9

Chung, Y.-C. (1976). A Deep ^{226}Ra Maximum in the Northeast Pacific. *Earth Planet Sci. Lett.* 32, 249–257. doi: 10.1016/0012-821X(76)90065-0

Chung, Y.-C., and Craig, H. (1980). ^{226}Ra in the Pacific Ocean. *Earth Planet Sci. Lett.* 49, 267–292. doi: 10.1016/0012-821X(80)90072-2

Church, T. M., and Wolgemuth, K. (1972). Marine Barite Saturation. *Earth Planet. Sci. Lett.* 15, 35–44.

Cortes, M. Y., Bollmann, J., and Thierstein, H. R. (2001). Coccolithophore Ecology at the HOT Station ALOHA, Hawaii. *Deep-Sea Res. II* 48, 1957–1981. doi: 10.1016/S0967-0645(00)00165-X

Dehairs, F., Baeyens, W., and Goeyens, L. (1992). Accumulation of Suspended Barite at Mesopelagic Depths and Export Production in the Southern Ocean. *Science* 258, 1332–1335. doi: 10.1126/science.258.5086.1332

Dehairs, F., Chesselet, R., and Jedwab, J. (1980). Discrete Suspended Particles of Barite and the Barium Cycle in the Open Ocean. *Earth Planet Sci. Lett.* 49, 528–550. doi: 10.1016/0012-821X(80)90094-1

Dehairs, F., Goeyens, L., Stroobants, N., Bernard, P., Goyet, C., Poisson, A., et al. (1990). On Suspended Barite and the Oxygen Minimum in the Southern Ocean. *Global Biogeochem. Cycles* 4 (1), 85–102. doi: 10.1029/GB004i001p00085

Dehairs, F., Jacquet, S., Savoye, N., Van Mooy, B. A. S., Buesseler, K. O., Bishop, J. K. B., et al. (2008). Barium in Twilight Zone Suspended Matter as a Potential Proxy for Particulate Organic Carbon Remineralization: Results for the North Pacifi. *Deep Sea Res. Part II: Topical Stud. Oceanogr.* 55, 1673–1683 doi: 10.1016/j.dsr2.2008.04.020

Dehairs, F., Stroobants, N., and Goeyens, L. (1991). Suspended Barite as Tracer of Biological Activity in the Southern Ocean. *Mar. Chem.* 35, 399–410. doi: 10.1016/S0304-4203(09)90032-9

Foster, D. A., Staubwasser, M., and Henderson, G. M. (2004). ^{226}Ra and Ba Concentrations in the Ross Sea Measured With Multicollector ICP Mass Spectrometry. *Mar. Chem.* 87, 59–71. doi: 10.1016/j.marchem.2004.02.003

Ganeshram, R. S., François, R., Commeau, J., and Brown-Leger, S. L. (2003). An Experimental Investigation of Barite Formation in Seawater. *Geochim. Cosmochim. Acta* 67 (14), 2599–2605. doi: 10.1016/S0016-7037(03)00164-9

González-Muñoz, M. T., Fernández-Luque, B., Martínez-Ruiz, F., Ben Chekroun, K., Arias, J. M., Rodríguez-Gallego, M., et al. (2003). Precipitation of Barite by Myxococcus Xanthus: Possible Implications for the Biogeochemical Cycle of Barium. *Appl. Environ. Microbiol.* 69, 5722–5725. doi: 10.1128/AEM.69.9.5722-5725.2003

Honda, M. C. (2003). Biological Pump in the Northwestern North Pacific. *J. Oceanogr.* 59, 671–684. doi: 10.1023/B:JOCE.0000009596.57705.0c

Honda, M. C., Imai, K., Nojiri, Y., Hoshi, F., Sugawara, T., and Kusakabe, M. (2002). The Biological Pump in the Northwestern North Pacific Based on Fluxes and Major Component of Particulate Matter Obtained by Sediment Trap Experiments, (1997–2000). *Deep Sea Res. Part II* 49, 5595–5625. doi: 10.1016/S0967-0645(02)00201-1

Honda, M. C., Kawakami, H., Sasaoka, K., Watanabe, S., and Dickey, T. (2006). Quick Transport of Primary Produced Organic Carbon to the Ocean Interior. *Geophys. Res. Lett.* 33, 1-4. doi: 10.1029/2006GL026466

Horner, T. J., Kinsley, C. W., and Nielsen, S. G. (2015). Barium-Isotopic Fractionation in Seawater Mediated by Barite Cycling and Oceanic Circulation. *Earth Planet Sci. Lett.* 430, 511–522. doi: 10.1016/j.epsl.2015.07.027

Hsieh, Y.-T., and Henderson, G. M. (2017). Barium Stable Isotopes in the Global Ocean: Tracer of Ba Inputs and Utilization. *Earth Planet Sci. Lett.* 473, 269–278. doi: 10.1016/j.epsl.2017.06.024

Jacquet, S. H. M., Dehairs, F., Dumont, I., Becquevort, S., Cavagna, A.-J., and Cardinal, D. (2011). Twilight Zone Organic Carbon Remineralization in the Polar Front Zone and Subantarctic Zone South of Tasmania. *Deep Sea Res. Part II Top. Stud. Oceanogr.* 58, 2222–2234. doi: 10.1016/j.dsr2.2011.05.029

Jacquet, S. H. M., Dehairs, F., Savoye, N., Obernosterer, I., Christaki, U., Monnin, C., et al. (2008). Mesopelagic Organic Carbon Mineralization in the Kerguelen Plateau Region Tracked by Biogenic Particulate Ba. *Deep-Sea Res. II* 55, 868–879. doi: 10.1016/j.dsr2.2007.12.038

Jacquet, S. H. M., Henjes, J., Dehairs, F., Worobiec, A., Savoye, N., and Cardinal, D. (2007). Particulate Ba-Barite and Acantharians in the Southern Ocean During the European Iron Fertilization Experiment (EIFEX). *J. Geophys. Res.* 112, G04006. doi: 10.1029/2006JG000394

Karl, D. M., and Lukas, R. (1996). The Hawaii Ocean Time-Series (HOT) Program: Background, Rationale and Field Implementation. *Deep-Sea Res. II* 43, 129–156. doi: 10.1016/0967-0645(96)00005-7

Kaufman, A., Trier, R. M., Broecker, W. S., and Feely, H. W. (1973). Distribution of 228Ra in the World Ocean. *J. Geophys. Res.* 78 (36), 8827–8848. doi: 10.1029/JC078i036p08827

Kawakami, H., and Kusakabe, M. (2008). Surface Water Mixing Estimated From ^{228}Ra and ^{226}Ra in the Northwestern North Pacific. *J. Environ. Radioact.* 99, 1335–1340. doi: 10.1016/j.jenvrad.2008.04.011

Ku, T.-L., Huh, C.-A., and Chen, P. S. (1980). Meridional Distribution of ^{226}Ra in the Eastern Pacific Along GEOSECS Cruise Tracks. *Earth Planet Sci. Lett.* 49, 293–308. doi: 10.1016/0012-821X(80)90073-4

Ku, T.-L., and Lin, M.-C. (1976). ^{226}Ra Distribution in the Antarctic Ocean. *Earth Planet Sci. Lett.* 32, 236–248. doi: 10.1016/0012-821X(76)90064-9

Ku, T.-L., and Luo, S. (1994). New Appraisal of Radium-226 as a Large-Scale Oceanic Mixing Tracer. *J. Geophys. Res.* 99, 255–210. doi: 10.1029/94JC00089

Lam, P. J., and Bishop, J. K. B. (2008). The Continental Margin is a Key Source of Iron to the HNLC North Pacific Ocean. *Geophys. Res. Lett.* 35 (7), 1–5. doi: 10.1029/2008gl033294

Lea, D. W., and Boyle, E. A. (1989). Barium Content of Benthic Foraminifera Controlled by Bottom-Water Composition. *Nature* 338, 751–753. doi: 10.1038/338751a0

Lea, D. W., and Boyle, E. A. (1990). A 210,000-Year Record of Barium Variability in the Deep Northwest Atlantic Ocean. *Nature* 347, 269–272. doi: 10.1038/347269a0

Legeleux, F., and Reyss, J.-L. (1996). Ra-228/ Ra-226 Activity Ratio in Oceanic Settling Particles : Implications Regarding the Use of Barium as a Proxy for Paleoproductivity Reconstruction. *Deep-Sea Res. I* 43 (11-12), 1857–1863. doi: 10.1016/S0967-0637(96)00086-6

Le Roy, E., Sanial, V., Charette, M. A., van Beek, P., Lacan, F., Jacquet, S., et al. (2018). Study of the 226Ra-Ba Relationship Along the GA01-GEOTRACES Section in the North Atlantic. *Biogeosciences* 15 (9), 3027–3048. doi: 10.5194/bg-15-3027-2018

Li, Y. H., Ku, T. L., Mathieu, G. G., and Wolgemuth, K. (1973). Barium in the Antarctic Ocean and Implications Regarding the Marine Geochemistry of Ba and ^{226}Ra. *Earth Planet Sci. Lett.* 19, 352–358. doi: 10.1016/0012-821X(73)90085-X

Martinez-Ruiz, F., Paytan, A., Gonzalez-Munoz, M. T., Jroundi, F., Abad, M. M., Lam, P. J., et al. (2020). Barite Precipitation on Suspended Organic Matter in the Mesopelagic Zone. *Front. Earth Sci.* 8. doi: 10.3389/feart.2020.567714

Michaels, A. F. (1988). Vertical Distribution and Abundance of Acantharia and Their Symbionts. *Mar. Biol.* 97, 559–569. doi: 10.1007/BF00391052

Michaels, A. F., Caron, D. A., Swanberg, N. R., Howse, F. A., and Michaels, C. (1995). Planktonic Sarcodines (Acantharia, Radiolaria, Foraminifera) in Surface Waters Near Bermuda: Abundance, Biomass and Vertical Flux. *J. Plankton Res.* 17 (1), 131–163. doi: 10.1093/plankt/17.1.131

Millero, F.J. (2005). Chemical Oceanography (*3rd eds.*). *CRC Press.* doi: 10.1201/9780429258718

Monnin, C. (1999). A Thermodynamic Model for the Solubility of Barite and Celestite in Electrolyte Solutions and Seawater From 0 to 200°C and to 1kbar. *Chem. Geol.* 153, 187–209. doi: 10.1016/S0009-2541(98)00171-5

Monnin, C., and Cividini, D. (2006). The Saturation State of the World's Ocean With Respect to (Ba,Sr)SO_4 Solid Solutions. *Geochim. Cosmochim. Acta* 70, 3290–3298. doi: 10.1016/j.gca.2006.04.002

Monnin, C., and Galinier, C. (1988). The Solubility of Celestite and Barite in Electrolyte Solutions and Natural Waters at 25°C. A Thermodynamic Study. *Chem. Geol.* 71-, 283–296 doi: 10.1016/0009-2541(88)90055-1

Monnin, C., Jeandel, C., Cattaldo, T., and Dehairs, F. (1999). The Marine Barite Saturation State of the World's Oceans. *Mar. Chem.* 65, 253–261. doi: 10.1016/S0304-4203(99)00016-X

Moore, W. S., and Dymond, J. (1991). Fluxes of Ra-226 and Barium in the Pacific Ocean : The Importance of Boundary Processes. *Earth Planet Sci. Lett.* 107, 55–68. doi: 10.1016/0012-821X(91)90043-H

Moore, W. S., Key, R. M., and Sarmiento, J. L. (1985). Techniques for Precise Mapping of 226Ra and 228Ra in the Ocean. *J. Geophys. Res.* 90, 6983–6995. doi: 10.1029/JC090iC04p06983

Moore, W. S., and Reid, D. F. (1973). Extraction of Radium From Natural Waters Using Manganese-Impregnated Acrylic Fibers. *J. Geophys. Res.* 78, 8880–8886. doi: 10.1029/JC078i036p08880

Oka, E., Qiu, B., Takatani, Y., Enyo, K., Sasano, D., Kosgi, N., et al. (2015). Decadal Variability of Subtropical Mode Water Subduction and its Impact on Biogeochemistry. *J. Oceanogr.* 71, 389–400. doi: 10.1007/s10872-015-0300-x

Paytan, A., Moore, W. S., and Kastner, M. (1996). Sedimentation Rate as Determined by ^{226}Ra Activity in Marine Barite. *Geochim. Cosmochim. Acta* 60 (22), 4313–4319. doi: 10.1016/S0016-7037(96)00267-0

Qiu, B., Chen, S., Schneider, N., and Taguchi, B. (2014). A Coupled Decadal Prediction of the Dynamic State of the Kuroshio Extension System. *J. Clim.* 27, 1751–1764. doi: 10.1175/JCLI-D-13-00318.1

Reyss, J.-L., Schmidt, S., Legeleux, F., and Bonte, P. (1995). Large, Low Background Well-Type Detectors for Measurements of Environmental Radioactivity. *Nucl. Inst. Meth. A* 357, 391–397. doi: 10.1016/0168-9002(95)00021-6

Rhein, M., and Schlitzer, R. (1988). Radium-226 and Barium Sources in the Deep East Atlantic. *Deep-Sea Res.* 35 (9), 1499–1510. doi: 10.1016/0198-0149(88)90099-4

Rushdi, A., McManus, J., and Collier, R. (2000). Marine Barite and Celestite Saturation in Seawater. *Mar. Chem.* 69, 19–31. doi: 10.1016/s0304-4203(99)00089-4

Schmidt, S., and Cochran, J. K. (2010). Radium and Radium-Daughter Nuclides in Carbonates: A Brief Overview of Strategies for Determining Chronologies. *J. Environ. Radioact.* 101, 530–537. doi: 10.1016/j.jenvrad.2009.10.006

Staubwasser, M., Henderson, G. M., Berkman, P. A., and Hall, B. L. (2004). Ba, Ra, Th, and U in Marine Mollusc Shells and the Potential of 226Ra/Ba Dating of Holocene Marine Carbonate Shells. *Geochim. Cosmochim. Acta* 68 (1), 89–100. doi: 10.1016/S0016-7037(03)00279-5

Sternberg, E., Tang, D., Tung-Yuan, H., Jeandel, C., and Morel, F. (2005). Barium Uptake and Adsorption in Diatoms. *Geochim. Cosmochim. Acta* 69, 2745–2752. doi: 10.1016/j.gca.2004.11.026

Stroobants, N., Dehairs, F., Goeyens, L., Vanderheijden, N., and van Grieken, R. (1991). Barite Formation in the Southern Ocean Water Column. *Mar. Chem.* 35, 411–421. doi: 10.1016/S0304-4203(09)90033-0

van Beek, P., François, R., Conte, M., Reyss, J.-L., Souhaut, M., and Charrette, M. (2007). $^{228}Ra_{ex}/^{226}Ra_{ex}$ and $^{226}Ra_{ex}$/Ba Ratios to Track Barite Formation and Transport in the Water Column. *Geochim. Cosmochim. Acta* 71, 71–86. doi: 10.1016/j.gca.2006.07.041

van Beek, P., and Reyss, J.-L. (2001). ^{226}Ra in Marine Barite: New Constraints on Supported ^{226}Ra. *Earth Planet Sci. Lett.* 187, 147–161. doi: 10.1016/S0012-821X(01)00288-6

van Beek, P., Reyss, J.-L., Bonte, P., and Schmidt, S. (2003). Sr/Ba in barite: a proxy of barite preservation in marine sediments? *Mar. Geol.* 199, 205–220 doi: 10.1016/S0025-3227(03)00220-2

van Beek, P., Reyss, J.-L., DeMaster, D., and Paterne, M. (2004). ^{226}Ra-in Marine Barite : Relationship With Carbonate Dissolution and Sediment Focusing in the Equatorial Pacific. *Deep-Sea Res. I* 51, 235–261. doi: 10.1016/j.dsr.2003.10.007

van Beek, P., Reyss, J.-L., Gersonde, R., Paterne, M., Rutgers van der Loeff, M., and Kuhn, G. (2002). ^{226}Ra in Barite : Absolute Dating of Holocene Southern Ocean Sediments and Reconstruction of Sea-Surface Reservoir Ages. *Geology* 30 (8), 731–734 doi: 10.1130/0091-7613(2002)030<0731:RIBADO>2.0.CO;2

van Beek, P., Souhaut, M., Lansard, B., Bourquin, M., Reyss, J.-L., Jean, P., et al. (2013). LAFARA : A New Underground Laboratory in the French Pyrénées for Low-Background Gamma Spectrometry. *J. Environ. Radioact.* 116, 152–158. doi: 10.1016/j.jenvrad.2012.10.002

van Beek, P., Souhaut, M., and Reyss, J.-L. (2010). Measuring the Radium Quartet (^{226}Ra, ^{228}Ra, ^{224}Ra, ^{223}Ra) in Water Samples Using Gamma Spectrometry. *J. Environ. Radioact.* 101, 521–529. doi: 10.1016/j.jenvrad.2009.12.002

van Beek, P., Sternberg, E., Reyss, J.-L., Souhaut, M., Robin, E., and Jeandel, C. (2009). ^{228}Ra/^{226}Ra and ^{226}Ra/Ba Ratios in the Western Mediterranean Sea: Barite Formation and Transport in the Water Column. *Geochim. Cosmochim. Acta* 73, 4720–4737. doi: 10.1016/j.gca.2009.05.063

Weast, R. C., Selby, S. M., and Hodgman, C. D. (1966). *Handbook of Chemistry and Physics. 46th edition* (Cleveland: the chemical rubber co), 1713 pp.

Wolgemuth, K., and Broecker, W. S. (1970). Barium in Sea Water. *Earth Planet Sci. Lett.* 8, 372–378. doi: 10.1016/0012-821X(70)90110-X

Conflict of Interest: The authors declare that the research was conducted in the absence of any commercial or financial relationships that could be construed as a potential conflict of interest.

Publisher's Note: All claims expressed in this article are solely those of the authors and do not necessarily represent those of their affiliated organizations, or those of the publisher, the editors and the reviewers. Any product that may be evaluated in this article, or claim that may be made by its manufacturer, is not guaranteed or endorsed by the publisher.